Journal of Alloys and Compounds 480 (2009) 161–166

Contents lists available at ScienceDirect

Journal of Alloys and Compounds

journal homepage: www.elsevier.com/locate/jallcom

Milling and subsequent thermal annealing effects on the microstructural and magnetic properties of nanostructured $Fe_{90}Co_{10}$ and $Fe_{65}Co_{35}$ powders

M. Delshad Chermahini [a], H. Shokrollahi [b,*]

[a] Department of Metallurgy, School of Engineering, Shahid Bahonar University of Kerman, P.O. Box No. 76135-133, Kerman, Iran
[b] Department of Materials Science and Engineering, Shiraz University of Technology, P.O. Box No. 71555-313 Shiraz, Iran

ARTICLE INFO

Article history:
Received 7 December 2008
Received in revised form 18 January 2009
Accepted 24 January 2009
Available online 6 February 2009

Keywords:
Nanostructured materials
Mechanical alloying
Microstructure
Magnetic measurements

ABSTRACT

The influence of milling and subsequent annealing on the microstructural and magnetic properties of $Fe_{90}Co_{10}$ and $Fe_{65}Co_{35}$ alloys is investigated. After milling for 8 h a body-centred cubic nanostructured Fe–Co alloy forms with an average crystallite size of about 12 nm. The magnetization saturation (M_S) increases ~16% for $Fe_{65}Co_{35}$ and 5% for $Fe_{90}Co_{10}$ alloys by milling for 8 h. Subsequent annealing of $Fe_{90}Co_{10}$ and $Fe_{65}Co_{35}$ powders for 105 min at 550 °C improves the M_S about 6 and 11%, respectively. Before annealing, the coercivity increases (up to 60 Oe) by milling for 3 h, followed by a reduction on milling for longer periods (45 h). At the initial stage of the heating, a sharp decrease in H_C to 8–10 Oe occurs due to the relief of internal strain. Further heating leads to an increase in the coercivity (intermediate times) followed by a slight diminution on heating for final stage.

1. Introduction

It is established that during mechanical alloying a solid state reaction takes place between the fresh powder surfaces of the reactant materials at room temperature. Consequently, it can be useful to produce alloys and compounds that are difficult and impossible to be obtained by conventional melting and casting techniques [1].

In general, due to the continuous severe plastic deformation, a gradual refinement of the internal structure of the powders to nanometer scales occurs during high-energy milling [2]. As a result some magnetic properties can be improved; while the presence of stresses and defects introduced by mechanical alloying deteriorate the magnetic property. For this reason, annealing process for the elimination of residual stresses is required [3,4].

The Fe–Co alloys have low coercive field, hysteresis loss, eddy current loss, high electric permeability and good saturation magnetization. Pure iron (bcc) offers a little more magnetic permeability than the iron–cobalt alloys. Pure Fe has been used in relays, solenoids and magnets in vacuum equipments, particularly in direct current magnetic field applications [5,6]. The potential of nanostructured alloys as modern soft magnetic materials relies on this fact that for grain size below a critical value, the coercivity (H_C) decreases rapidly ($H_C \propto D^6$) with decreasing grain size, as predicted by Random Anisotropy Model [7]. According to this model, when the grain size is smaller than magnetic exchange length, the soft magnetic properties in the nanostructured materials are ascribed to the averaging out the magneto-crystalline anisotropy due to the random distribution of the nano-scale grain [8].

This paper focuses on the investigation of influence of the milling and subsequent annealing on microstructural and magnetic properties of $Fe_{90}Co_{10}$ and $Fe_{65}Co_{35}$ alloys which have been less investigated.

2. Experimental details

Fe (99.5%, <10 μm) and Co (99%, <3 μm) powders supplied by *Merck* were mechanically alloyed in an argon atmosphere to form $Fe_{1-x}Co_x$ alloy in a *Fritsch* planetary ball mill, while confined in sealed 250 ml steel containers rotated at 400 rpm for a variety of milling times (0, 3, 8, 20, 35 and 45 h). The container was loaded with a blend of balls (φ = 10 mm, mass = 4.14 g and φ = 20 mm, mass = 32.12 g). The number of used balls was 12 and 18 for φ = 20 and 10 mm, respectively. The total weight of the powder was about 23 g and the ball to powder mass ratio was about 20:1. In order to minimize contamination, the wear-resistant steel balls and container were used. The powders were vacuum encapsulated in quartz cylinders then annealed at different times (15, 30, 45, 60, 75, 90 and 105 min) and temperatures (450 and 550 °C). X-ray diffraction measurements were carried out in a *Philips X'Pert High Score* diffractometer using Cu Kα (λ = 1.5405 Å) radiation over 20–140° 2θ. To adjust the shift of zero angle, the silicon crystal used as a standard sample. The crystallite size and lattice strain were estimated using the Williamson–Hall method [9,10]:

$$B_s \cos\theta = 2(\varepsilon) \sin\theta + \frac{k\lambda}{D} \quad (1)$$

where B_s is the full-width at half maximum of the diffraction peak, θ is the Bragg angle, ε is the internal microstrain λ is the wavelength of the X-ray, D is the crystallite size. B_s can be given as:

$$B_s^2 = B_m^2 - B_c^2 \quad (2)$$

* Corresponding author. Tel.: +98 711 7354520; fax: +98 711 7354520.
E-mail address: shokrollahi@sutech.ac.ir (H. Shokrollahi).

0925-8388/$ – see front matter © 2009 Elsevier B.V. All rights reserved.
doi:10.1016/j.jallcom.2009.01.088

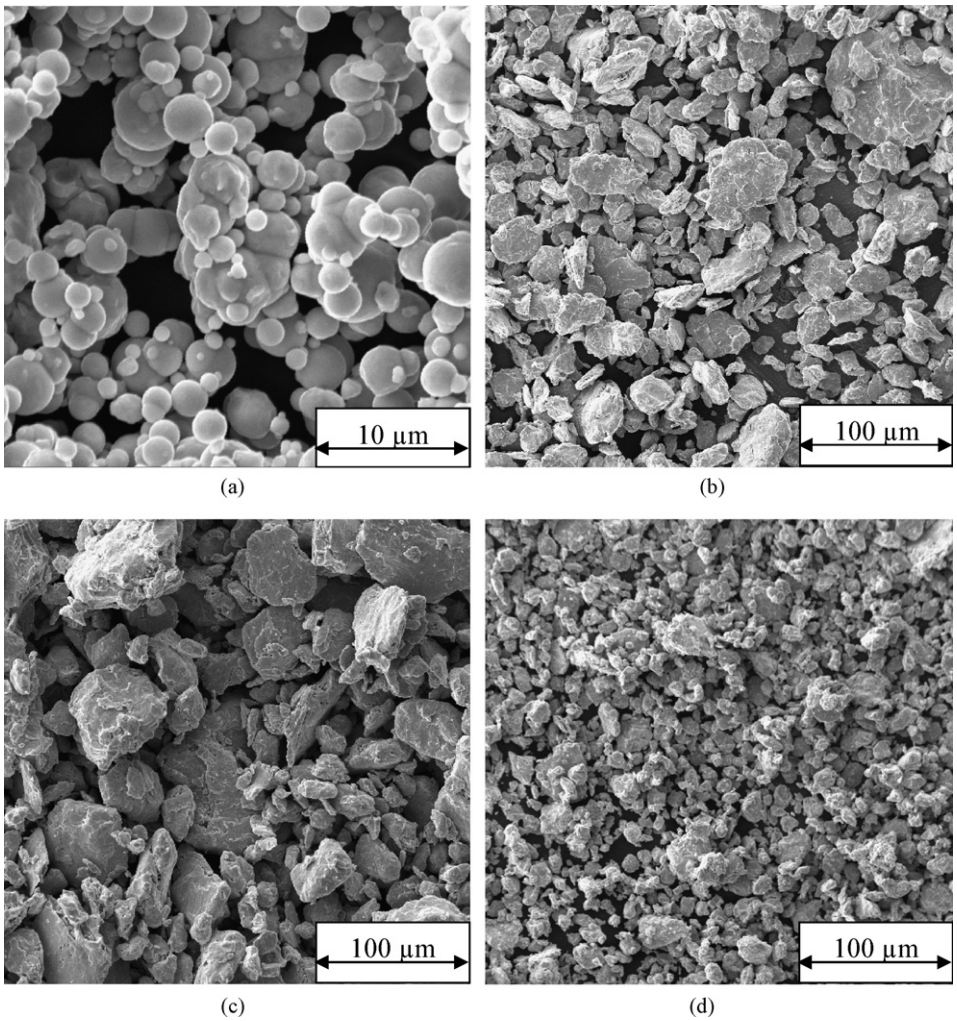

Fig. 1. SEM micrographs of pure Fe and $Fe_{90}Co_{10}$ powders for various milling times. (a) Pure Fe, t = 0 h, (b) $Fe_{90}Co_{10}$, t = 3 h; (c) $Fe_{90}Co_{10}$, t = 8 h and (c) $Fe_{90}Co_{10}$, t = 35 h.

where B_s is the width at half maximum of the Si powder peaks used for calibration and B_m is the evaluated width. Lattice parameters were determined using 3 high-angle peaks in order to increase the precision of the measurements. Morphology and particle size were observed using scanning electron microscopy (*Camscan mv2300*). Magnetic properties were estimated at room temperature using a vibrating sample magnetometer (VSM) at a field of 0.95 T.

3. Results and discussion

3.1. Morphology

During the milling of ductile–ductile systems the powders are repeatedly flattened, cold welded, fractured and rewelded [11].

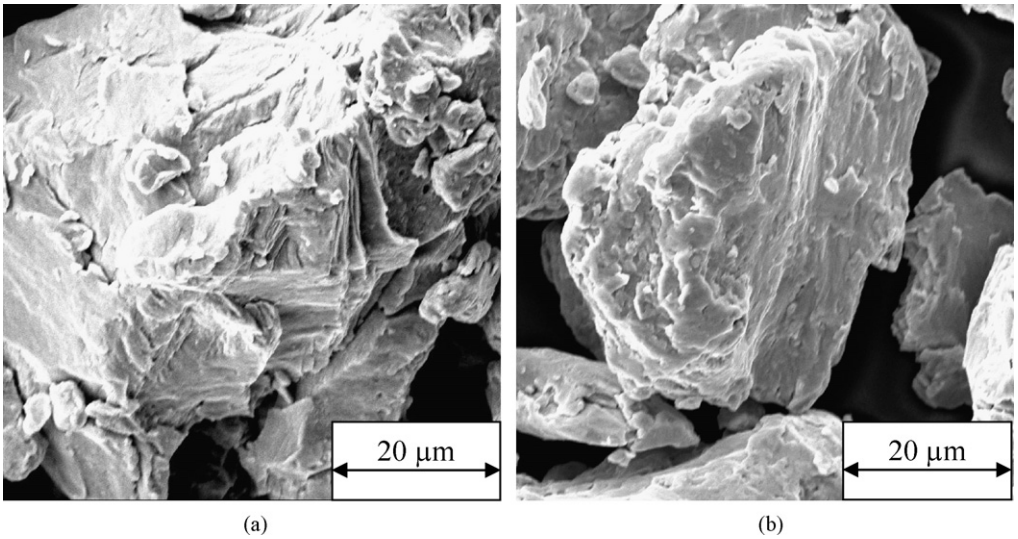

Fig. 2. High magnification SEM micrographs of $Fe_{90}Co_{10}$ powders for various milling times. (a) t = 8 h; (b) t = 35 h.

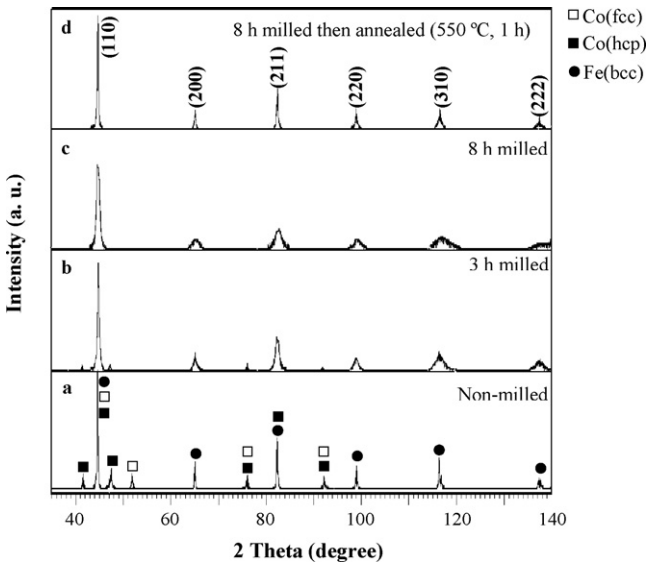

Fig. 3. Evolution of XRD patterns with milling and thermal annealing for $Fe_{65}Co_{35}$ powder mixtures. (a) Unmilled; (b) 3 h milled; (c) 8 h milled; (d) 8 h milled then annealed at 550 °C for 1 h.

Fig. 1 depicts the spherical shapes of the micrometer sized powder particle prior to milling; subsequent to milling for 3 h, the spheres are flattened (Fig. 1a). With further milling, the powder size and particle shape have a wide distribution. The mean particle size increases because the propensity for welding exceeds that for fracture (Fig. 1b). After 8 h of milling, the lamellar structure due to welding of different particles becomes evident (Fig. 1c). Prolonged milling results in a narrower distribution of particle sizes as a balance is reached between the fracture and welding processes (Fig. 1d) [12].

As shown in Fig. 2a by milling for 8 h, the lamellar structure formed for $Fe_{90}Co_{10}$. It has been established that the thickness and number of layer in each particle can affect the alloying treatment [13]. After milling for 35 h (Fig. 2b), the lamellar structure disappeared, completely which can be an evidence for the chemical homogeneity of the crystalline grains.

3.2. Microstructure

Fig. 3 shows the evolution of XRD patterns with milling and annealing time. Non-milled powders show the presence of body-centred cubic iron (bcc), hexagonal close-packed (hcp) cobalt and face-centred cubic (fcc) cobalt (Fig. 3a). The Co diffraction peaks (hcp and fcc) completely disappear after 8 h, corresponding to the onset of alloy formation with iron (Fig. 3c). Additionally, milling treatment leads to the expected broadening of the bcc Fe–Co peaks due to refinement and the existence of heterogeneous strains [13]. Conversely, annealing returns the peak width and height approximately to that of the non-milled powders (Fig. 3d) indicating an increase in crystallite size associated with a strain relief.

Fig. 4a and b illustrates the crystallite size evolution on milling and annealing time, respectively. In the beginning, mechanical alloying leads to a rapid decrease in the crystallite size (less than 20 nm) for all compositions. Further refinement occurs slowly to about 12 nm after extended milling (20 h). The decrease of the crystallite size with milling time is attributed to dislocation generation caused by severe plastic deformation [14]. In addition, on the basis of the coherent polycrystal model [15,16], the volume fraction of the grain boundaries f_{gb} was estimated on the formula

$$f_{gb} = 1 - f_g \tag{3}$$

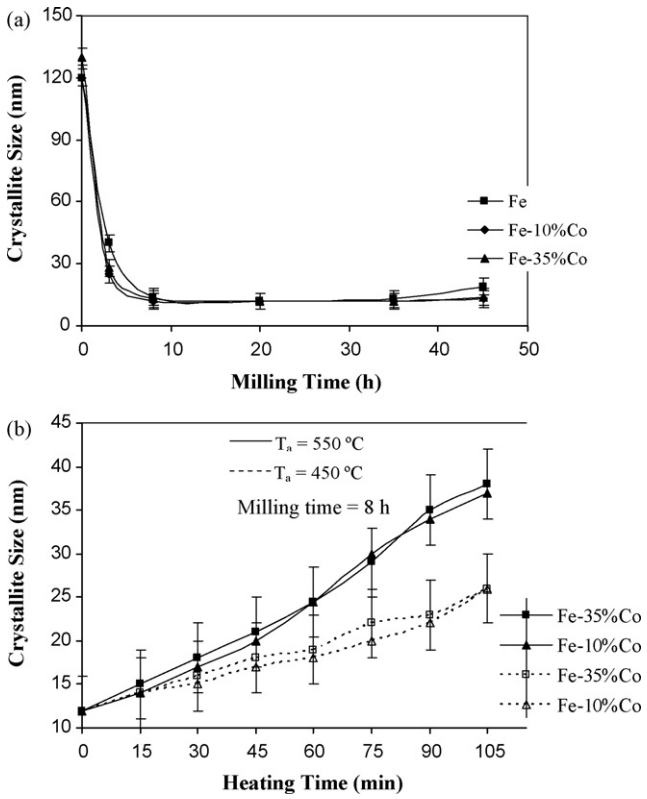

Fig. 4. Evolution of crystallite size with (a) milling time; (b) annealing time for different annealing temperatures (T_a).

where f_g denotes the volume fraction of the grains given by

$$f_g = \frac{(D-d)^3}{D^3} \tag{4}$$

and D is the crystallite size, d is the effective grain-boundary thickness. In most of the nanostructured alloys, the estimated thickness of the interfaces was roughly found at 2–3 atomic layers that is physically consistent with the thickness of the surface layer encountered in non-interacting nanoparticle systems [15,17]. The values of f_{gb} are about 18 and 6% for D = 12 nm (after 8 h milling) and 40 nm (after 105 min annealing at 550 °C), respectively. On thermal annealing, the final crystallite size (<40 nm) is found to be lower than in starting powders (120 nm) and the alloy retains its nanostructured state (Fig. 4b).

Fig. 5 shows the effect of milling and subsequent annealing treatment on the lattice strain. The lattice strain increases by milling for 8 h due to severe plastic deformation then retains constant (up to 35 h). The small decrease in microstrain associated with 35–45 h of milling is attributed to the temperature rise during prolonged milling [11]. As shown in Fig. 5b, the lattice strain produced by milling is removed by annealing for 15 and 30 min at 550 and 450 °C, respectively.

Fig. 6a shows that for pure Fe and Fe in $Fe_{90}Co_{10}$ powder mixtures, with further milling the lattice parameter increases due to the heavily cold worked and plastically deformed state of powders [18]. Generally, in nanostructured materials, the lattice expansion may be caused by defects introduced in interfaces. The less dense structure of interfaces can result in some negative pressure on the interfaces [19] and this can lead to an increase in lattice parameter. On the other hand, the lattice parameter decreases for $Fe_{65}Co_{35}$ alloys (up to 8 h). This latter may be due to allotropic phase transformation of Co (fcc–hcp) and/or to the triple defect disorder [1,11,18]. This type of disorder has been observed in the Co alloys

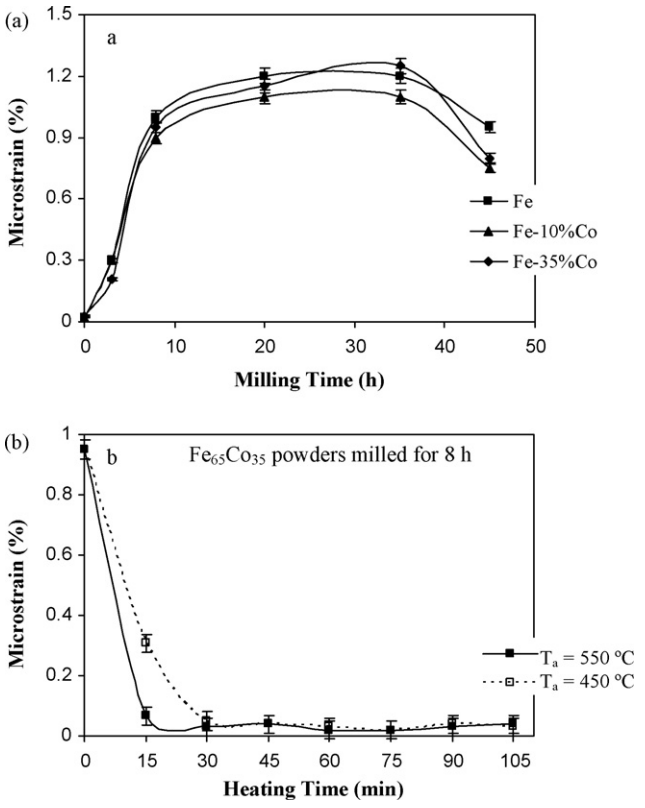

Fig. 5. Evolution of microstrain with (a) milling time; (b) annealing time for different annealing temperatures (T_a).

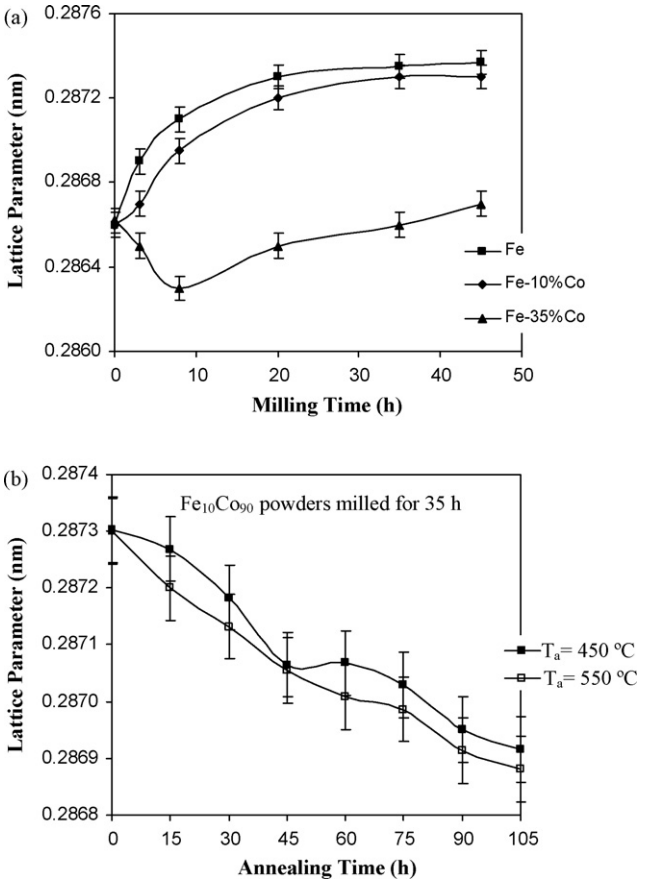

Fig. 6. Evolution of lattice parameter with (a) milling time; (b) annealing time for different annealing temperatures (T_a).

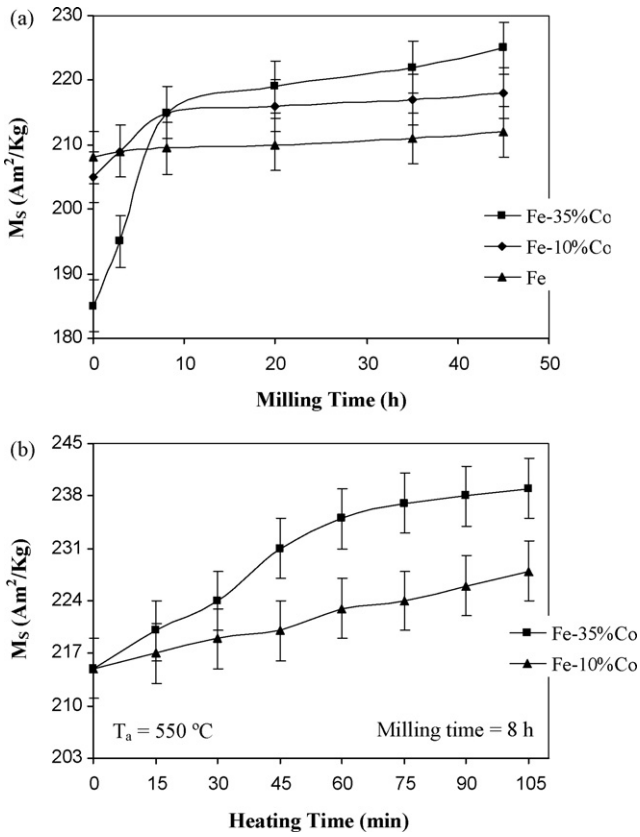

Fig. 7. M_S of Fe–Co powder mixtures versus (a) milling times; (b) heating times for different annealing temperatures (T_a).

prepared by mechanical alloying such as B2 CoGa and B2 CoAl. The so-called triple defect consists of one anti-site Co atom combined with two vacancies on the Co sub-lattice [18]. In addition, for $Fe_{65}Co_{35}$ powders, the unexpected increase of lattice parameter (8–45 h) may be due to the complex stochastic and selfhood nature of MA process [20] or probably to the effect of cumulative plastic deformation which is dominant. As shown in Fig. 6b, with increasing the heating time the lattice parameter decreases due to the decrease in interfaces caused by grain growth during heating.

3.3. Magnetic studies

As shown in Fig. 7, for the non-milled Fe–Co powder mixtures, the M_S is close to the weighted average of the M_S of pure Fe and Co powders. The magnetization saturation increases ~16% for $Fe_{65}Co_{35}$ and 5% for $Fe_{90}Co_{10}$ alloys by milling for 8 h due to the completion of alloying process. The increase of M_S during milling can be ascribed to the completion of alloying and the diminution in magneto-crystalline anisotropy due to the grain refinement [3], which leads to an easier rotation of the magnetic vector. The grain refinement diminishes the magneto-crystalline anisotropy due to the averaging effect of magnetization over randomly oriented nano-sized grains [3]. At low grain sizes, each grain may be treated as a single magnetic domain eliminating the influence from magnetic walls [5]. The powders, which milled for 8 h and then annealed for 105 min at 550 °C, improve the M_S from 215 A m^2/kg (non-annealed powders) to 228–240 A m^2/kg (Fig. 5b). The increased numbers of dislocation and other lattice defects cause this change [21]. The resulting microstress impedes both domain wall motion and domain rotation. Depending on the temperature, two main phenomena [20] occur, which both can increase the M_S.

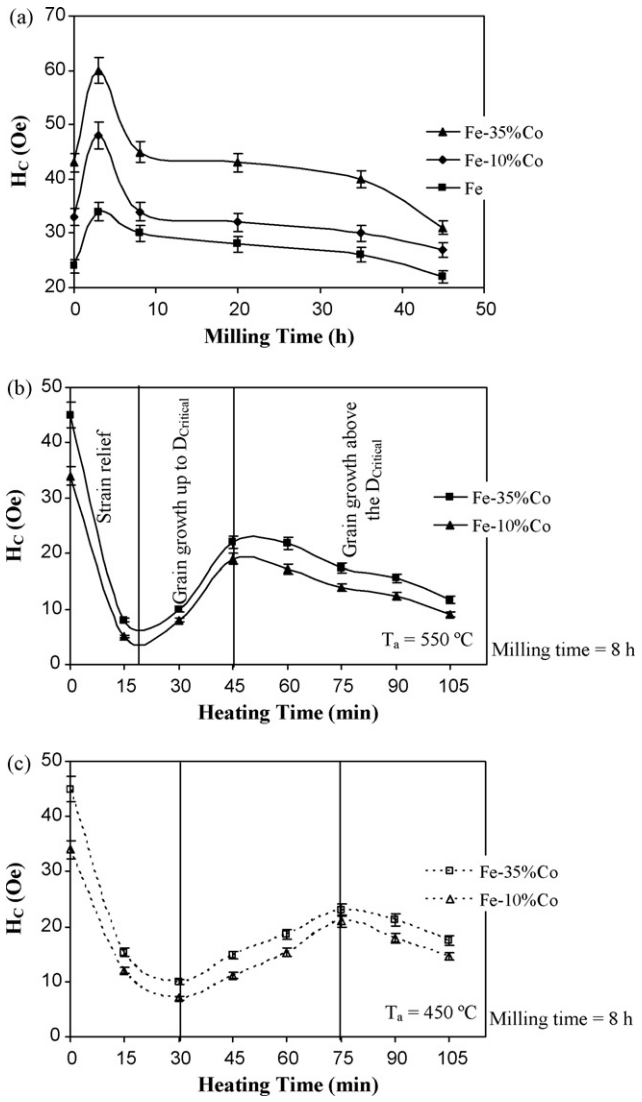

Fig. 8. Evolution of H_C with (a) milling time, (b) annealing time at 550 °C and (c) annealing time at 450 °C.

(a) Recrystallization (400–500 °C), the cold-worked material (microstrain ~1%) is replaced by stress-free ones, which leads to a moderate increase in M_S.
(b) Grain growth (>500 °C), the new stress-free grains grow, the atomic fraction of grain boundaries (f_{gb}) decreases from 18% for 8 h milled alloy to ~6% for annealed powders (105 min at 550 °C). It permits easier motion of domain walls and leads to a noticeable increase in M_S.

Fig. 8 depicts the milling and heating time dependence of H_C for FeCo powders. On milling, the H_C reaches a maximum (60 and 48 Oe for $Fe_{65}Co_{35}$ and $Fe_{90}Co_{10}$ powders, respectively) at 3 h due to the grain refinement and introduction of the microstrain into the material [4]. In the early stages, the grain size exceeds the domain wall thickness and as a result, the grain boundaries act as impediments to domain wall motion and increase the H_C. Recent work [22] has led to the realization that for small grain size H_C decreases rapidly with decreasing grain size when the domain wall exceeds the grain size. It seems that from 3 to 35 h the coercivity diminishes due to the effect of the very small grain size [23], which overwhelms the effect of microstrains. From 35 to 45 h the coercivity decreases due to the temperature rise effect during long milling times [11], which can slightly anneal the internal strain. Minimum of H_C (22 Oe) achieves

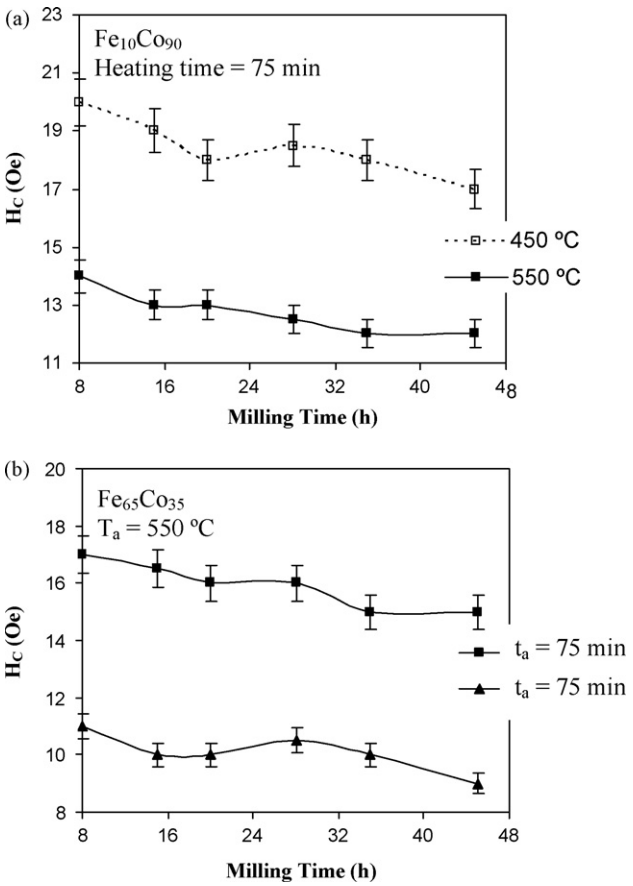

Fig. 9. H_C versus milling time for (a) $Fe_{90}Co_{10}$ powders annealed 75 min at different annealing temperatures (T_a); (b) $Fe_{65}Co_{35}$ powders annealed at 550 °C for different heating times (t_a).

by milled Fe for 45 h while maximum values (60 Oe) observes for $Fe_{65}Co_{35}$ after 3 h milling. On annealing, three stages are observed (Fig. 8b and c). At short heating times, the coercivity decreases considerably after heat treatment for 15 and 30 min at 550 and 450 °C, respectively through the relief of internal strain. This effect of thermal annealing on the H_C can be confirmed by the nucleation field's theory [24]. According to this theory, H_C for a nucleation type magnet can be written as:

$$H_C = cH_A - N_dM_S \quad (5)$$

where H_A is the anisotropy field of the magnetic phase, c is the constant, N_d is the demagnetizing factor and M_S is the saturation magnetization. This equation shows that the effective anisotropy field influences the value of coercivity. Anisotropy field is a function of microstrain and increasing the microstrain increases the anisotropy field via increasing the strain anisotropy. For intermediate annealing times, H_C shows a remarkable increase by heating for 45 and 75 min at 550 and 450 °C, respectively. With increasing crystallite size D the coercivity steeply increases following a D^6-power [5] (up to $D_{Critical}$ = 20 nm). At the final stage, with increasing the heating time, crystallite size exceeds $D_{Critical}$. As a result, a slight reduction in the coercivity is observed [22,25]. All stages shift to the long heating times for powders annealed at 450 °C (Fig. 8b) compared with that in 550 °C (Fig. 8c).

Fig. 9 shows the H_C of annealed powders versus milling time for different heating times (Fig. 9a) and temperatures (Fig. 9b). The milling time before annealing has no remarkable effect on the coercivity of annealed powders. It can be a consequence of similar microstructure (crystallite size and microstrain) obtained by milling for 8–45 h. On the other hand, the H_C for elevated annealing

time and temperature decreases due to the increase in the crystallite size.

4. Conclusions

The high-energy milling and subsequent thermal annealing is a promising method to prepare nanostructured soft magnetic powders such as Fe and Fe–Co alloys, which possess low coercivity and high saturation magnetization. From this study, the following conclusions could be drawn. Indeed the reduction in grain size leads to a noticeable increase in interfaces fraction which results in a soft magnetic behavior of the materials.

(1) Within the first 8 h of milling, the dramatic increase in the microstrain (up to 1%) and the reduction of the crystallite size (<20 nm) due to the dislocation generation are observed. conversely, annealing leads to a diminution of the lattice strain (0.02%) and an increase in the crystallite size (up to 38 nm).
(2) With further milling, for pure Fe and Fe in $Fe_{90}Co_{10}$ powder mixtures, the lattice parameter increases due to the heavily cold worked and plastically deformed state of powders. On the other hand, the lattice parameter decreases for $Fe_{65}Co_{35}$ alloys (up to 8 h). This latter may be due to allotropic phase transformation of Co (fcc–hcp) and/or to the triple defect disorder. On annealing, with increasing the heating time the lattice parameter decreases due to the decrease in interfaces caused by grain growth during heating.
(3) By milling for 3 h, the coercivity reaches a maximum (60 and 48 Oe for $Fe_{90}Co_{10}$ and $Fe_{65}Co_{35}$ powders, respectively) due to the introduction of the strain and defects and to the reduction of crystallite size from 120 to 20 nm. By milling for 3–35 h, the coercivity reduces (to 40 and 30 Oe for $Fe_{65}Co_{35}$ and $Fe_{90}Co_{10}$ powders, respectively) due to the effect of very fine crystallite size (<20 nm). For long milling times, H_C decreases slightly due to the stress relief caused by temperature rise effect during long period of milling. On annealing, 3 stages are observed. At the initial stage, the coercivity diminishes to 8–10 Oe due to the strain relief. For middle stage, a quick increase in the H_C (up to 20 Oe) due to the increase in the crystallite size (<20 nm) occurs. Long heating times lead to a slight decrease in the H_C (to ~12 Oe) due to the grain growth (>20 nm).
(4) By milling for 8 h, the M_S shows a significant increase (16% for $Fe_{65}Co_{35}$ and 5% for $Fe_{90}Co_{10}$ alloys) due to the completion of alloying and then shows a slight increase from 8 to 45 h due to the reduction of magneto-crystalline anisotropy caused by the grain refinement. The powders, which milled for 8 h and then annealed for 105 min at 550 °C, improve the M_S to 240–250 A m^2/kg.

Finally, the best way to get FeCo alloys with better soft magnetic properties is the milling of $Fe_{65}Co_{35}$ powders for 8 h and subsequent annealing for 105 min at 550 °C. This way results in 238–A m^2/kg and ~10 Oe for saturation magnetization and coercivity, respectively.

Acknowledgements

I am thankful to my friends Mr. M. Mirzaee and Mr. H. Montazeri for their assistances. Some magnetic measurements were performed at the Magnetic Research Lab. Group, Kashan University, which is appreciated.

References

[1] M. Sherif El-Eskandarani, Mechanical Alloying for Fabrication of Advanced Engineering Materials, William Andrew, 2001, p. 2.
[2] Carl C. Koch, Nanostructured Materials Processing, Properties and Potential Applications, William Andrew, 2002, p. 76.
[3] H. Shokrollahi, S. Sharafi, R. Koohkan, K. Janghorban, J. Magn. Magn. Mater. 320 (2008) 1089–1094.
[4] H. Shokrollahi, K. Janghorban, J. Magn. Magn. Mater. 317 (2007) 61–67.
[5] Y. Liu, J. Zhang, L. Yu, G. Jia, Y. Zhang, Curr. Appl. Phys. 4 (2004) 455–460.
[6] H. Shokrollahi, K. Janghorban, J. Mater. Process. Technol. 189 (2007) 1–12.
[7] G. Herzer, IEEE Trans. Magn. 26 (1990) 1390–1397.
[8] N.E. Fenineche, R. Hamzaoui, O. Elkedim, Mater. Lett. 57 (2003) 4165–4169.
[9] B.D. Cullity, Elements of X-ray Diffraction, 2nd ed., Addison-Wesley, 1978, p. 356.
[10] G.K. Williamson, W.H. Hall, Acta Metall. 1 (1953) 22–31.
[11] C. Suryanarayana, Prog. Mater. Sci. 46 (2001) 1–184.
[12] Y.D. Kim, J.Y. Chung, J. Kim, H. Jeon, Mater. Sci. Eng. A 291 (2000) 17–21.
[13] B. Lee, B.S. Ahn, D.G. Kim, S.T. Oh, H. Jeon, J. Ahn, Y.D. Kim, Mater. Lett. 57 (2003) 1103–1107.
[14] J.R. Ares, F. Cuevas, Acta Mater. 53 (2005) 2157–2167.
[15] H.W. Song, S.R. Guo, Z.Q. Hu, Nanostruct. Mater. 11 (1999) 203.
[16] T. Pikula, D. Oleszak, J. Magn. Magn. Mater. 320 (2008) 413–420.
[17] J.M. Greneche, A. S' lawska-Waniewska, J. Magn. Magn. Mater. 264 (2000) 215–216.
[18] H. Moumeni, S. Alleg, J.M. Greneche, J. Alloys Compd. 386 (2005) 12–19.
[19] William A. Goddard, Donald W. Brenner, Handbook of Nanoscience, Engineering and Technology, CRC Press, 2003, pp. 590–630.
[20] C. Suryanarayana, E. Ivanov, V.V. Boldyriv, Mater. Sci. Eng. A 304–306 (2001) 151–158.
[21] B.D. Cullity, Introduction to Magnetism and Magnetic Materials, Addisson Wesely Publishing Company, 1972.
[22] Michael E. McHenry, Matthew A. Willard, David E. Laughlin, Prog. Mater. Sci. 44 (1999) 291–433.
[23] R. Hamzaoui, O. Elkedim, N. Fenineche, E. Gaffet, J. Craven, Mater. Sci. Eng. A 360 (2003) 299–305.
[24] G. Herzer, W. Fernegel, E. Adler, J. Magn. Magn. Mater. 58 (1986) 48.
[25] T. Sourmail, Scripta Mater. 51 (2004) 589–591.